Identification of excited states in ^{125}Ce

E. S. Paul,[1] A. J. Boston,[1] A. Galindo-Uribarri,[2] T. N. Ginter,[3] C. J. Gross,[2,4] A. N. James,[1] P. J. Nolan,[1] R. D. Page,[1] S. D. Paul,[2] A. Piechaczek,[5] D. C. Radford,[2] W. Reviol,[6] L. L. Riedinger,[6] H. C. Scraggs,[1] W. Weintraub,[6] and C.-H. Yu[2]

[1]*Oliver Lodge Laboratory, University of Liverpool, Liverpool L69 7ZE, United Kingdom*

[2]*Physics Division, Oak Ridge National Laboratory, Oak Ridge, Tennessee 37831*

[3]*Department of Physics and Astronomy, Vanderbilt University, Nashville, Tennessee 37235*

[4]*Oak Ridge Institute for Science and Education, Oak Ridge, Tennessee 37831*

[5]*Department of Physics and Astronomy, Louisiana State University, Baton Rouge, Louisiana 70803*

[6]*Department of Physics and Astronomy, University of Tennessee, Knoxville, Tennessee 37996-1200*

(Received 19 March 1998)

Excited states have been identified in neutron-deficient $^{125}_{58}Ce_{67}$ using the ^{58}Ni(^{70}Ge,$2pn$)^{125}Ce reaction at 280 and 310 MeV. The experiment was performed at the Holifield Radioactive Ion Beam Facility, Oak Ridge National Laboratory. A γ-ray array of six clover plus four single-crystal HPGe detectors was used in conjunction with the Recoil Mass Spectrometer, which had a position sensitive avalanche counter (mass A identification) at its focal plane, together with an ionization chamber (charge Z identification). Two band structures assigned to ^{125}Ce are interpreted as based on the $\nu h_{11/2}[523]7/2^-$ and $\nu d_{5/2}[402]5/2^+$ Nilsson orbitals, respectively. [S0556-2813(98)03808-4]

PACS number(s): 27.60.+j, 23.20.Lv, 25.70.Gh

I. INTRODUCTION

Light cerium isotopes are of current interest in high-spin nuclear-structure physics because of the ''superdeformed'' shell gap that occurs for $Z=58$ at a quadrupole deformation $\beta_2 \sim 0.35-0.40$ (a prolate shape with an axis ratio of 3:2). The pertinent question is: can superdeformation solely arise from this proton shell gap or are deformation-driving neutron intruder orbitals ($\nu i_{13/2}$) [1,2] also required? This question may be addressed by searching for superdeformed bands in light cerium isotopes where the neutron intruders are too high above the Fermi surface to be populated, even at the highest spins experimentally attainable. In this regard, superdeformed bands are known in $^{129-134}$Ce [2–11] while ^{128}Ce is the lightest isotope currently showing evidence for superdeformation [12]. However, before high-spin studies for the lighter isotopes can be adequately performed with the new generation of highly efficient γ-ray spectrometers (e.g., GAMMASPHERE, EUROBALL [13]), it is vital to establish the low-spin level structures, into which the superdeformed bands will feed. Furthermore, the ground-state deformation trends of light cerium nuclei are of current interest; for instance, does the quadrupole deformation keep increasing as neutrons are removed (relative to the $N=82$ shell closure) or is a maximal value reached? Theory suggests a maximum ground-state deformation for cerium isotopes of $\beta_2 \approx 0.308$ just below mid-shell ($N \lesssim 66$) [14]. In view of these questions, studies of neutron-deficient cerium isotopes are highly topical.

Although excited states are currently known in the even $^{124}_{58}Ce_{66}$ [15] and $^{126}_{58}Ce_{68}$ [16] isotopes, $^{127}_{58}Ce_{69}$ [17] is the lightest odd-A isotope for which band structures have been published. The present study was therefore undertaken in order to identify transitions in light cerium isotopes and this report documents γ-ray transitions in $^{125}_{58}Ce_{67}$. Previous work [18] on ^{125}Ce has proposed an $I^\pi=5/2^+$ ground state by a comparison of relative γ-ray intensities in ^{124}Ba, produced through β-delayed proton decay, with statistical model calculations. Three low-energy transitions were proposed to feed this $I^\pi=5/2^+$ ground state following the β^+/EC decay of ^{125}Pr [19]. In addition, excited states in ^{125}Ce were proposed [20,21] following early work carried out at the Daresbury Nuclear Structure Facility, UK, during commissioning of the Recoil Separator [22]. The present results generally confirm the earlier results for ^{125}Ce.

II. EXPERIMENTAL DETAILS

The present results for ^{125}Ce were obtained as part of a preliminary investigation of neutron-deficient nuclei near $A=120$, using the ^{70}Ge+^{58}Ni heavy-ion fusion-evaporation reaction, performed at the Holifield Radioactive Ion Beam Facility (HRIBF), Oak Ridge National Laboratory. A ^{70}Ge beam was provided at energies 280, 310, 340, and 370 MeV, and used to bombard two self-supporting ^{58}Ni foils, of nominal thickness 500 μg/cm^2 each, over a period of three days. A complementary study using a ^{69}As radioactive beam, instead of the stable ^{70}Ge beam, is envisioned in the near future.

A preliminary set of experimental apparatus was available for the present study at HRIBF. Six four-element clover and four single-crystal HPGe detectors were placed around the target position, at a distance of 19 cm. The efficiency of all 28 separate HPGe elements was approximately 25% each relative to a standard 7.6 cm×7.6 cm Na(Tl) crystal at $E_\gamma=1.33$ MeV. Five of the clover detectors consisted of vertically segmented crystals, but none of the clover detectors had anticompton shielding. The four single-crystal detectors were however within bismuth germanate anticompton shields. Recoiling evaporation residues leaving the target foils were focused through the Recoil Mass Spectrometer (RMS) [23–25], which in this experiment provided a mass

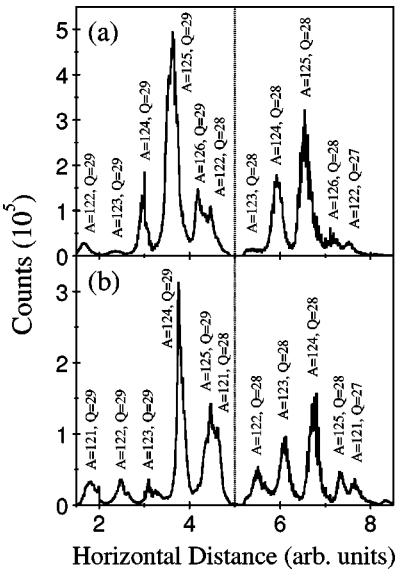

FIG. 1. PSAC spectra obtained for the ^{70}Ge+^{58}Ni reaction at 280 MeV (a) and 310 MeV (b). The dotted vertical line signifies that the PSAC consists of two distinct halves. The mass peaks are labeled by their A and Q values.

resolution $M/\Delta M \approx 350$. The RMS has acceptances of $\pm 10\%$ in recoil ion energy and $\pm 5\%$ in mass-to-charge ratio (A/Q). A Position Sensitive Avalanche Counter (PSAC) [25] was mounted at the RMS focal plane to provide mass identification, via the A/Q ratio, of spatially separated (horizontally) recoil products. The PSAC consisted of two electrically separated halves, wide enough to span two charge states of the recoils arriving at the focal plane. A split anode ionization chamber (IC), similarly consisting of two electrically separated halves, was mounted behind the PSAC providing total-energy (E) and energy-loss (ΔE) signals for Z discrimination. Conventional NIM-based electronics were used for all HPGe and ancillary detectors.

III. RESULTS

The results for ^{125}Ce were obtained from the data measured at beam energies of 280 and 310 MeV, using a γ-recoil trigger that required at least one HPGe detector in prompt time coincidence with a recoil signal from the PSAC. Horizontal projections of the PSAC are shown in Fig. 1, where the recoils are dispersed in terms of the A/Q ratio. The mass peaks are labeled by their A and Q values and it can be seen that mass $A=125$ dominates at 280 MeV [Fig. 1(a)], while mass $A=124$ dominates at 310 MeV [Fig. 1(b)]. Figure 2 shows a projection of the γ-ray data in coincidence with any recoil (a) and specific mass peaks (b)–(d) for the 280 MeV data; approximately 46% of the 3.9×10^6 γ-recoil events correspond to mass $A=125$. Similar γ-ray spectra are shown in Fig. 3 for the 310 MeV data. In this case, approximately 2.5% of the 2.3×10^6 γ-recoil events correspond to mass 125, while mass 124 accounts for 20%. Note that more γ-ray transitions appear in the 310-MeV data of Fig. 3 compared to the 280-MeV data of Fig. 2, since the average γ-ray fold per event is higher. While the average γ-ray fold is 2.09 for the 280-MeV data, it is 3.30 for the 310-MeV data.

In Fig. 2(d), transitions from ^{122}Ba [26] ($\alpha 2p$ exit channel) appear in this ''mass 126'' spectrum in addition to the expected transitions from ^{126}Ce [16] ($2p$). This is caused by a so-called ''charge-state ambiguity'' in the A/Q value that is dispersed by the RMS. The optimum charge state for recoils is $Q=29$, but since $A/Q \approx 4.0$, recoils with mass ($A-4$) and $Q=28$ may contaminate the $Q=29$ mass peaks (and similarly recoils with mass ($A-8$) and $Q=27$, etc.). This is indeed evident in Fig. 1(a) where the $A=126$, $Q=29$ peak (^{126}Ce) is not cleanly resolved from the $A=122$, $Q=28$ peak (^{122}Ba). A similar situation occurs for the $A=125$, $Q=29$ and $A=121$, $Q=28$ mass peaks in Fig. 1(b). It should be emphasized, however, that the RMS was set to accept values of A/Q for the recoils of interest ($A=125$ at 280 MeV, $A=124$ at 310 MeV) where charge-state ambiguities were not present. In view of the above comments, only the γ-recoil data recorded at 280 MeV were analyzed for the identification of ^{125}Ce. At this low beam energy, three-particle evaporation dominates [see Fig. 2(a)] and possible A/Q contamination from $A=121$ recoils (seven particles removed from the compound ^{128}Nd nucleus) is kept to a minimum. Moreover, γ-ray transitions in the possible $A=121$ contaminants are known [27].

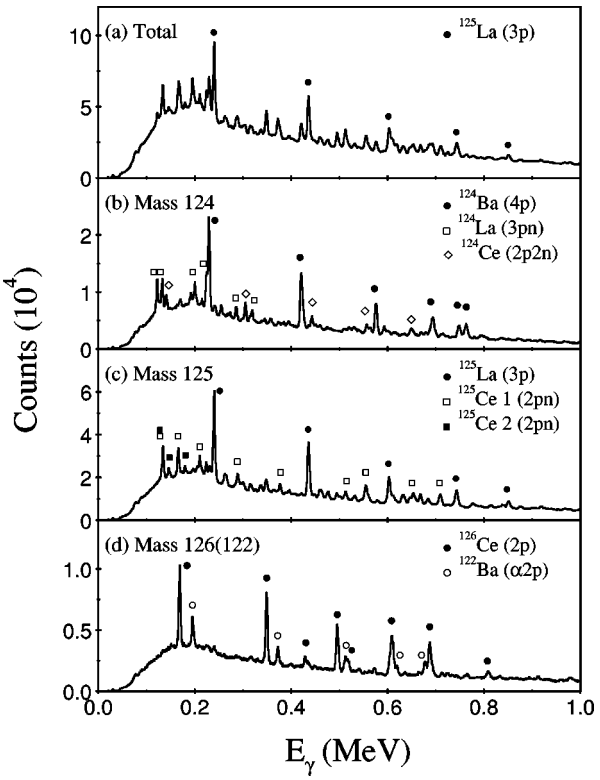

FIG. 2. Total γ-ray spectrum (a) in coincidence with any recoil for the ^{70}Ge+^{58}Ni reaction at 280 MeV. Mass-gated spectra for $A=124$, 125, and 126 are shown in (b)–(d), respectively. The strong transitions are denoted in each spectrum, including the ^{125}Ce transitions in (c). Note that contaminants from ^{122}Ba are evident in (d) due to a charge-state ambiguity in the A/Q values, as discussed in the text.

It can be seen in Fig. 2 that pure charged-particle evaporation channels dominate each of the mass-gated spectra. In addition, the strongest lines in the total spectrum, Fig. 2(a), belong to the $3p$ evaporation channel, namely ^{125}La [28]. The mass $A=125$ spectrum of Fig. 2(c) also has other relatively strong peaks labeled as ^{125}Ce; these peaks are approxi-

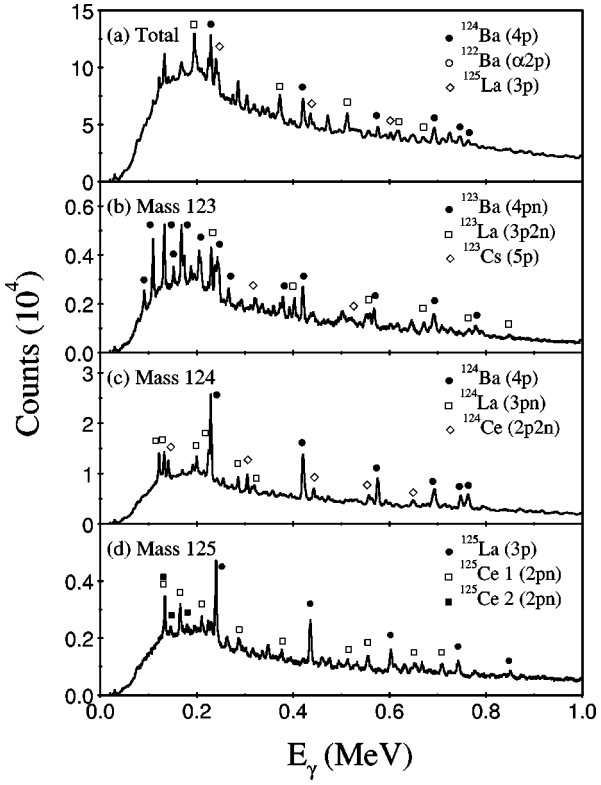

FIG. 3. Total γ-ray spectrum (a) in coincidence with any recoil for the ^{70}Ge+^{58}Ni reaction at 310 MeV. Mass-gated spectra for $A=123$, 124, and 125 are shown in (b)–(d), respectively. The strong transitions are denoted in each spectrum, including the ^{125}Ce transitions in (d).

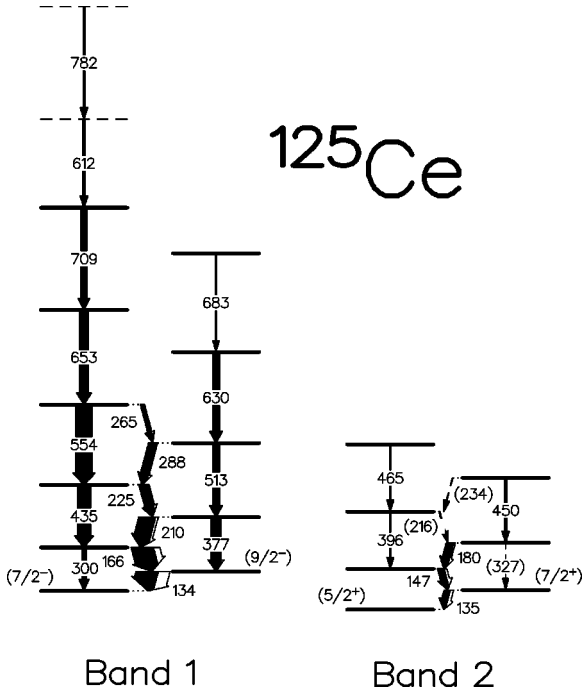

FIG. 4. Proposed level scheme for ^{125}Ce, with transition energies given in keV. The widths of the arrows are proportional to their total intensity, with the white parts showing the calculated component from internal conversion. The tentative spin/parity assignments of the lowest levels are taken from systematics, while the relative excitation energy of the band-heads is unknown.

mately one-third of the intensity of the ^{125}La transitions. From the systematic observation in Figs. 2 and 3 of pure proton evaporation (xp) being stronger than xpn evaporation, which is in turn stronger than $xp2n$ evaporation, it might be expected that the strongest peaks in Fig. 2(c) correspond to ^{125}La ($3p$) and ^{125}Ce ($2pn$), respectively. This observation is in reasonably good agreement with theoretical relative yields obtained with the fusion-evaporation code ALICE [29]; the $3p$, $2pn$, and $p2n$ channels are predicted to be populated in the ratio 16:8:1 at a beam energy of 280 MeV.

In order to investigate the coincidence relationships of the γ-ray transitions evident in Fig. 2(c), mass 125 gated $\gamma-\gamma$ coincidences were incremented into a 2D matrix for the data sets at both 280 and 310 MeV. This matrix, containing 5.5 million coincidences, was analyzed using the RADWARE graphical analysis package [30]. A level scheme of mutually coincident γ rays, not in coincidence with known ^{125}La transitions [28], but assigned to ^{125}Ce, is shown in Fig. 4 consisting of two band structures. Band 1 is assumed to consist of low-energy dipole transitions linking two $\Delta I=2$ sequences. Given the low statistics of the present data, it was not possible to measure angular correlations of the new transitions. Band 1 agrees with the earlier work of Ref. [20], except that two transitions, found to be contaminants from ^{125}La [28], have been removed from the main sequence. Contamination from ^{125}La occurs since several of the strongest transitions assigned to ^{125}Ce (166, 435, 554 keV) are doublets with transitions in sidebands of ^{125}La [28]. Examples of γ-ray coincidence spectra for Band 1 are shown in Fig. 5; the 653 keV spectrum shown in Fig. 5(b) represents the strongest clean gate available. Band 1 is easily identified up to the 709 keV transition, above which the sequence of γ rays becomes irregular. Weaker transitions of energies 612 and 782 keV are evident in Fig. 5, and may represent the continuation of Band 1 where an alignment of a quasiparticle pair is expected (see Sec. IV B). Their ordering is however unclear, and the topmost levels are therefore shown dashed in the level scheme of Fig. 4. Band 2 in Fig. 4 is weaker than Band 1; the lowest three (dipole) transitions are consistent with Ref. [19], while the bracketed transitions could not be confirmed here but are taken from Ref. [20].

In order to confirm the assignment of the new transitions to ^{125}Ce, the ratio of the IC total-energy and energy-loss signals ($E/\Delta E$) was investigated, gated by certain γ-ray transitions and A/Q values for $A=125$, from the data recorded at 280 MeV. It proved possible to gate on two mutually coincident γ-ray transitions (double gate) of Band 1 in addition to the mass gate, significantly cleaning the $E/\Delta E$ spectrum; this spectrum is shown in Fig. 6(a). For mass 125, any two γ rays were taken from the lists: 241, 435, 602, 743, 852, and 920 keV ($^{125}_{57}$La, known); and 134, 166, 210, 225, and 288 keV (Band 1 of $^{125}_{58}$Ce, proposed). The centroids of the $E/\Delta E$ distributions of Fig. 6(a) are measured as 27.81(4) for the known $^{125}_{57}$La transitions and 27.07(4) for the proposed $^{125}_{58}$Ce transitions. The centroids differ by 0.74 of a channel, which is however much larger than the statistical errors. Furthermore, the $E/\Delta E$ distribution for the new ^{125}Ce

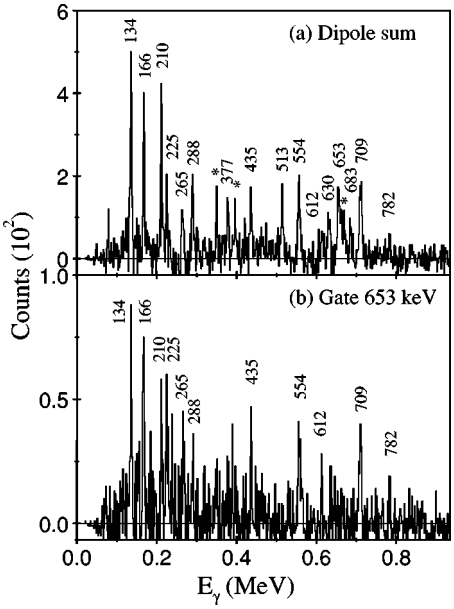

FIG. 5. Background-subtracted coincident γ-ray spectra for Band 1 of ^{125}Ce obtained from the mass $A=125$ gated $\gamma-\gamma$ matrix. A sum of gates set on the 134, 166, 210, 225, 288, and 265 keV dipole transitions (a), and a single gate set on the 653 keV transition (b), are shown. Transitions of Band 1 are labeled by their energies in keV, while contaminants from ^{125}La are denoted by asterisks.

transitions is consistently higher (lower) than the ^{125}La distribution at the left (right) of Fig. 6(a). This suggests that the distributions indeed arise from recoils with different Z values and hence Band 1 can be assigned to ^{125}Ce with some confidence. It should be noted that the ionization chamber provides much better Z discrimination for lighter nuclei ($A \leqslant 100$) and for higher recoil velocities (here $v/c \sim 4-5\%$)

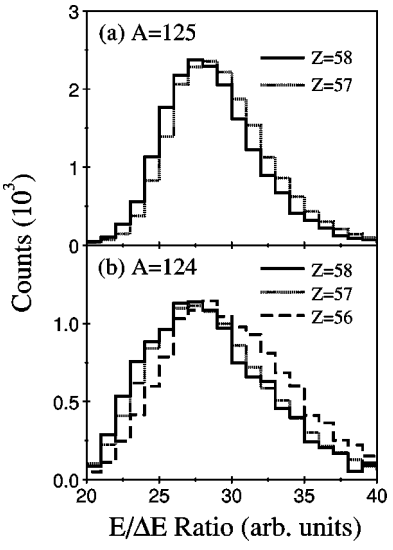

FIG. 6. Normalized $E/\Delta E$ distributions for $A=125$ recoils from the 280 MeV data (a). These distributions are also double gated by γ rays from known ^{125}La (dotted) and proposed ^{125}Ce (solid). Similar $E/\Delta E$ distributions for $A=124$ recoils from the 310 MeV data are shown in (b).

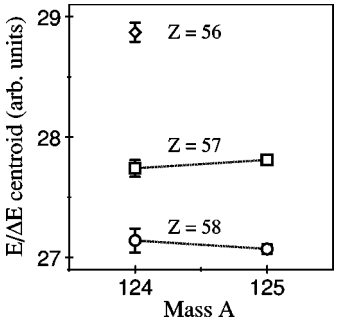

FIG. 7. Measured centroids of $E/\Delta E$ distributions for nuclei with $Z=56$, 57, and 58.

than the present experiment [31]. The weakness, and limited number of transitions, of Band 2 precluded a similar analysis of the $E/\Delta E$ distribution for this band. Hence the present data can only identify Band 2 with mass 125 and the explicit assignment to ^{125}Ce is therefore based on the results of Refs. [19–21].

To further investigate the sensitivity of the $E/\Delta E$ distributions with regard to Z discrimination for the present experiment, a similar analysis was applied to the $A=124$ recoils from the data recorded at a beam energy of 310 MeV. In this case, double γ-ray gates were taken from a list of transitions appropriate for $^{124}_{56}$Ba [32], $^{124}_{57}$La [33], and $^{124}_{58}$Ce [15], respectively. The resulting $E/\Delta E$ distributions are shown in Fig. 6(b), where again the centroids differ for each Z value. In this case, values of 28.87(8), 27.74(7), and 27.14(10) were found, respectively, for $^{124}_{56}$Ba, $^{124}_{57}$La, and $^{124}_{58}$Ce. Again, a small but significant difference is found for each Z, and the values for the La and Ce isobars are consistent with values for the corresponding $A=125$ isobars. The results of the measured centroids are shown graphically in Fig. 7.

IV. DISCUSSION

A. Band assignments

Systematics suggest that Band 1 of ^{125}Ce is based on the negative-parity $\nu h_{11/2}[523]7/2^-$ Nilsson orbital and that Band 2 is based on the positive-parity $\nu d_{5/2}[402]5/2^+$ Nilsson orbital with the $I=\Omega=5/2$ level representing the ground state of ^{125}Ce. These two orbitals are known to lie close together in both the ^{127}Ce isotope [17] and the ^{123}Ba isotone [34]. Band 1 in ^{125}Ce is the most developed with the favored $\alpha=-1/2$ signature branch observed to the highest spin. The quadrupole transition energies of this band are lower than the corresponding transitions in ^{127}Ce [17], which are in turn lower than those of ^{129}Ce [2,35]. This indicates that the quadrupole deformation increases for this series of odd-N isotopes as more neutrons are removed, consistent with theory [14]. Furthermore, the energy splitting between the two signature branches in Band 1 of ^{125}Ce is smaller than that of the corresponding band in ^{127}Ce, which is in turn smaller than that of ^{129}Ce. This again indicates that the deformation increases with decreasing neutron number. This energy splitting is shown schematically in Fig. 8(a) which plots the staggering parameter, defined as

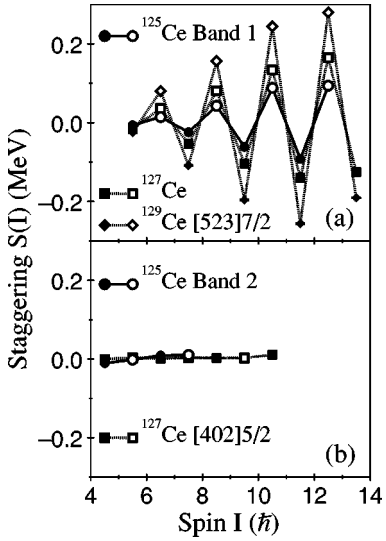

FIG. 8. Plot of the energy staggering parameter $S(I)$ versus spin I for bands in ^{125,127,129}Ce.

$$S(I)=E(I)-E(I-1)$$

$$-\frac{1}{2}[E(I+1)-E(I)+E(I-1)-E(I-2)], \quad (1)$$

as a function of spin for ^{125,127,129}Ce. Similar plots are shown in Fig. 8(b) for Band 2 of ^{125}Ce and the corresponding band in ^{127}Ce. In this case, the energy splitting is vanishingly small, consistent with a $\nu d_{5/2}(\Omega=j=5/2)$ assignment.

$B(M1;I\rightarrow I-1)/B(E2;I\rightarrow I-2)$ ratios of reduced transition probabilities may be readily extracted from experimental γ-ray branching ratios of competing $\Delta I=1$ and $\Delta I=2$ transitions. Such ratios have been extracted for Band 1 of ^{125}Ce, as shown in Fig. 9. The ratios average around a value of 1.0 $(\mu_N/eb)^2$. Theoretical estimates, using the Dönau and Frauendorf semiclassical formalism [36,37], are also shown in the figure assuming different Nilsson orbitals derived from the $\nu h_{11/2}$ midshell. The experimental results are consistent with that expected for the $[523]7/2^-$ assignment.

B. Alignment properties

The alignment, i_x [38], of Band 1 in ^{125}Ce is shown in Fig. 10 as a function of rotational frequency, ω, where it is

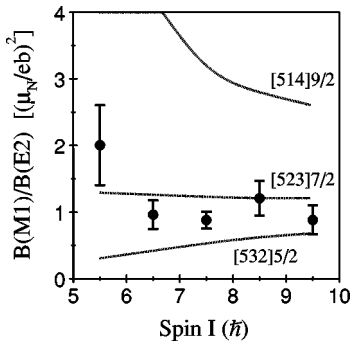

FIG. 9. Experimental (circles) and theoretical (lines) $B(M1)/B(E2)$ ratios of reduced transition probabilities for Band 1 in ^{125}Ce.

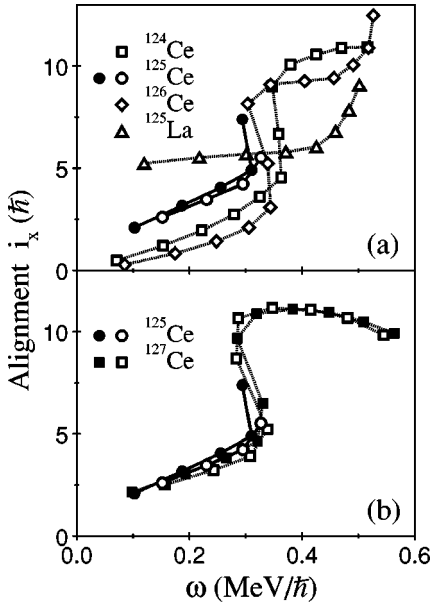

FIG. 10. Experimental alignments for ^{125}Ce Band 1, compared to the yrast bands of ^{124,126}Ce and ^{125}La (a), and ^{127}Ce (b).

compared to those of the yrast bands of even ^{124}Ce [15], ^{126}Ce [16], and odd-Z ^{125}La [28] [Fig. 10(a)], and odd-N ^{127}Ce [17] [Fig. 10(b)]. A rotational reference, based on a configuration with a variable moment of inertia, $\mathcal{J}_{\rm ref}=\mathcal{J}_0+\omega^2\mathcal{J}_1$, has been subtracted in each case with Harris parameters [39] $\mathcal{J}_0=14.1\hbar^2$ MeV^{-1} and $\mathcal{J}_1=38.4\hbar^4$ MeV^{-3}; the S band of ^{132}Ce over the frequency range $0.30\leqslant\omega\leqslant0.60$ MeV/$\hbar$ was used as the reference [40] for this systematic comparison. Note that the published yrast bands of ^{125}La [28] and ^{126}Ce [16] have each been extended by one γ-ray transition from the present work. In addition, three further γ-ray transitions have been added to the yrast band of ^{126}Ce following state-of-the-art four-dimensional (γ^4: ''hypercube'') RADWARE analysis [30] of a recent EUROBALL experiment [12] where ^{126}Ce was populated very weakly via the ^{100}Mo(^{32}S,$6n\gamma$) reaction.

An increase in i_x is observed in the yrast bands of ^{124,126}Ce at a rotational frequency $\omega\sim0.35$ MeV/$\hbar$, which may be attributed to the rotational alignment of $h_{11/2}$ protons by comparison with standard cranking calculations. This is indeed corroborated by the behavior of the yrast band (single $h_{11/2}$ proton) of ^{125}La where this proton alignment is Pauli blocked. The i_x pattern for ^{125}Ce starts to upbend at a similar frequency to those of ^{124,126}Ce and ^{127}Ce, again suggesting the onset of $h_{11/2}$ proton rotational alignment. Furthermore, the later upbends at $\omega\sim0.50$ MeV/$\hbar$ in ^{126}Ce and ^{125}La may be attributed to the rotational alignment of $h_{11/2}$ neutrons, since this alignment is Pauli blocked in the case of ^{127}Ce which already contains a single $h_{11/2}$ neutron.

V. CONCLUSIONS

Employing an array of HPGe detectors in conjunction with the Recoil Mass Separator at HRIBF, transitions have been assigned to ^{125}Ce using the ^{70}Ge+^{58}Ni reaction. Two band structures have been identified: one is proposed to be

built on the $I^{\pi}=5/2^{+}$ ground state associated with a $\nu d_{5/2}$ orbital, while the second is associated with a negative-parity $\nu h_{11/2}$ orbital. Systematic properties of the latter band are consistent with it being based on the $[523]7/2^{-}$ Nilsson orbital. The level spacings of this band also imply a larger quadrupole deformation than the heavier ^{127}Ce isotope.

ACKNOWLEDGMENTS

This work was partly supported by the U.S. Department of Energy under Contracts No. DE-AC05-96OR22464, ORISE DE-AC05-76OR00033, and by the U.K. Engineering and Physical Sciences Research Council (EPSRC). A.J.B. and H.C.S. acknowledge financial support from the EPSRC.

[1] R. Wyss, J. Nyberg, A. Johnson, R. Bengtsson, and W. Nazarewicz, Phys. Lett. B **215**, 211 (1988).
[2] A. Galindo-Uribarri, S. M. Mullins, D. Ward, M. Cromaz, J. DeGraaf, T.E. Drake, S. Flibotte, V.P. Janzen, D.C. Radford, and I. Ragnarsson, Phys. Rev. C **54**, R454 (1996).
[3] J.N. Wilson, G.C. Ball, M. Cromaz, T.E. Drake, S. Flibotte, A. Galindo-Uribarri, J. DeGraaf, G. Hackman, S.M. Mullins, J.M. Nieminen, V.P. Janzen, D.C. Radford, J.C. Waddington, and D Ward, Phys. Rev. C **55**, 519 (1997).
[4] A.T. Semple, E.S. Paul, A.J. Boston, I.M. Hibbert, D.T. Joss, P.J. Nolan, N.J. O'Brien, C.M. Parry, S.L. Shepherd, R. Wadsworth, and R. Wyss, J. Phys. G **24**, 1125 (1998).
[5] Y.-X. Luo, J.-Q. Zhong, D.J.G. Love, A. Kirwan, P.J. Bishop, M.J. Godfrey, I. Jenkins, P.J. Nolan, S.M. Mullins, and R. Wadsworth, Z. Phys. A **A329**, 125 (1988).
[6] A.T. Semple, P.J. Nolan, C.W. Beausang, S.A. Forbes, E.S. Paul, J.N. Wilson, R. Wadsworth, K. Hauschild, R.M. Clark, C. Foin, J. Genevey, J. Gizon, A. Gizon, J.A. Pinston, D. Santos, B.M. Nyáko, L. Zolnai, W. Klamra, and J. Simpson, Phys. Rev. C **54**, 425 (1996).
[7] P.J. Nolan, A.J. Kirwan, D.J.G. Love, A.H. Nelson, D.J. Unwin, and P.J. Twin, J. Phys. G **11**, L17 (1985).
[8] A.J. Kirwan, G.C. Ball, P.J. Bishop, M.J. Godfrey, P.J. Nolan, D.J. Thornley, D.J.G. Love, and A.H. Nelson, Phys. Rev. Lett. **58**, 467 (1987).
[9] D. Santos, J. Gizon, C. Foin, J. Genevey, A. Gizon, M. Józsa, J.A. Pinston, C.W. Beausang, S.A. Forbes, P.J. Nolan, E.S. Paul, A.T. Semple, J.N. Wilson, R.M. Clark, K. Hauschild, R. Wadsworth, J. Simpson, B.M. Nyakó, L. Zolnai, W. Klamra, N. El Aouad, and J. Dudek, Phys. Rev. Lett. **74**, 1708 (1995).
[10] K. Hauschild, R. Wadsworth, R.M. Clark, P. Fallon, D.B. Fossan, I.M. Hibbert, A.O. Macchiavelli, P.J. Nolan, H. Schnare, A.T. Semple, I. Thorslund, L. Walker, W. Satula, and R. Wyss, Phys. Lett. B **353**, 438 (1995).
[11] N.J. O'Brien *et al.* (private communicaton).
[12] E.S. Paul *et al.*, Euroball Experiment EB97.03 (unpublished).
[13] C.W. Beausang and J. Simpson, J. Phys. G **22**, 527 (1996).
[14] P. Möller, J.R. Nix, W.D. Myers, and W.J. Swiatecki, At. Data Nucl. Data Tables **59**, 185 (1995).
[15] K.L. Ying, P.J. Bishop, A.N. James, A.J. Kirwan, D.J.G. Love, T.P. Morrison, P.J. Nolan, D.C.B. Watson, K.A. Connell, A.H. Nelson, and J. Simpson, J. Phys. G **12**, L211 (1986).
[16] R. Moscrop, M. Campbell, W. Gelletly, L. Goettig, C.J. Lister, and B.J. Varley, Nucl. Phys. **A481**, 559 (1988).
[17] B.M. Nyakó, J. Gizon, V. Barci, A. Gizon, S. Andre, D. Barneoud, D. Curien, J. Genevey, and J.C. Merdinger, Z. Phys. A **A334**, 513 (1989).
[18] P.A. Wilmarth, J.M. Nitschke, R.B. Firestone, and J. Gilat, Z. Phys. A **A325**, 485 (1986).
[19] A. Osa, M. Asai, M. Koizumi, T. Sekine, S. Ichikawa, Y. Kojima, H. Yamamoto, and K. Kawade, Nucl. Phys. **A588**, 185c (1995).
[20] K.L. Ying, Ph.D. thesis, University of Liverpool, 1986.
[21] K.L. Ying, P.J. Bishop, A.N. James, A.J. Kirwan, T.P. Morrison, P.J. Nolan, D.C.B. Watson, K.A. Connell, D.J.G. Love, A.H. Nelson, and J. Simpson, *Nuclear Structure Appendix to the Daresbury Annual Report (1986/87)*, p. 27 (1987).
[22] A.N. James, T.P. Morrison, K.L. Ying, K.A. Connell, H.G. Price, and J. Simpson, Nucl. Instrum. Methods Phys. Res. A **267**, 144 (1988).
[23] J.D. Cole, T.M. Cormier, J.H. Hamilton, and A.V. Ramayya, Nucl. Instrum. Methods Phys. Res. B **70**, 343 (1992).
[24] C.J. Gross, T.N. Ginter, Y.A. Akovali, M.J. Brinkman, J.W. Johnson, J. Mas, J.W. McConnell, W.T. Milner, D. Shapira, and A.N. James, in *Proceedings of the 14th International Conference on the Application of Accelerators in Research and Industry, Denton, Texas, 1996*, edited by J.L. Duggan and I.L. Morgan, AIP Conf. Proc. No. 392 (AIP, New York, 1997) p. 401.
[25] C.J. Gross, Z. Phys. A **A358**, 249 (1997).
[26] T. Tamura, Nucl. Data Sheets **71**, 461 (1994), and references therein.
[27] T. Tamura, H. Iimura, K. Miyano, and S. Ohya, Nucl. Data Sheets **64**, 323 (1991), and references therein.
[28] K. Starosta, Ch. Droste, T. Morek, J. Srebrny, D.B. Fossan, D.R. LaFosse, H. Schnare, I. Thorslund, P. Vaska, M.P. Waring, W. Satula, S.G. Rohoziński, R. Wyss, I.M. Hibbert, R. Wadsworth, K. Hauschild, C.W. Beausang, S.A. Forbes, P.J. Nolan, and E.S. Paul, Phys. Rev. C **53**, 137 (1996).
[29] F. Plasil and M. Blann, Phys. Rev. C **11**, 508 (1975).
[30] D.C. Radford, Nucl. Instrum. Methods Phys. Res. A **361**, 297 (1995); **361**, 306 (1995).
[31] J.D. Garrett, Nucl. Phys. **A616**, 3c (1997).
[32] S. Pilotte, S. Flibotte, S. Monaro, N. Nadon, D. Prevost, P. Taras, H.R. Andrews, D. Horn, V.P. Janzen, D.C. Radford, D. Ward, J.K. Johansson, J.C. Waddington, T.E. Drake, A. Galindo-Uribarri, and R. Wyss, Nucl. Phys. **A514**, 545 (1990).
[33] T. Komatsubara, K. Furuno, T. Hosoda, J. Mukai, T. Hayakawa, T. Morikawa, Y. Iwata, N. Kato, J. Espino, J. Gascon, N. Gjorup, G.B. Hagemann, H.J. Jensen, D. Jerrestam, J. Nyberg, G. Sletten, B. Cederwall, and P.O. Tjom, Nucl. Phys. **A557**, 419c (1993).
[34] S. Ohya and T. Tamura, Nucl. Data Sheets **70**, 531 (1993), and references therein.
[35] Y. Tendow, Nucl. Data Sheets **77**, 631 (1996), and references therein.
[36] F. Dönau and S. Frauendorf, in *Proceedings of the Conference on High Angular Momentum Properties of Nuclei, Oak Ridge,*

1982, edited by N.R. Johnson (Harwood Academic, New York, 1983), p. 143.
[37] F. Dönau, Nucl. Phys. **A471**, 469 (1987).
[38] R. Bengtsson and S. Frauendorf, Nucl. Phys. **A327**, 139 (1979).
[39] S.M. Harris, Phys. Rev. **138**, B509 (1965).
[40] E.S. Paul, A.J. Boston, D.T. Joss, P.J. Nolan, J.A. Sampson, A.T. Semple, F. Farget, A. Gizon, D. Santos, B.M. Nyakó, N.J. O'Brien, C.M. Parry, and R. Wadsworth, Nucl. Phys. **A619**, 177 (1997).